23rd ABCM International Congress of Mechanical Engineering
December 6-11, 2015, Rio de Janeiro, RJ, Brazil

EXPERIMENTAL AND NUMERICAL STUDY OF THE PERFORMANCE CHARACTERISTICS OF A PICO HYDRO TURBINE MANUFACTURED BY INDALMA INDUSTRIES INC

Nigel M.D. Sloot
Ramsay Mac Donald
Nawin R. Nannan
Mechanical Engineering Discipline, Anton de Kom University of Suriname, Leysweg 86, PO Box 9212, Paramaribo, Suriname
slootnigel@gmail.com, ramsay_macdonald@yahoo.com, ryan.nannan@uvs.edu/ryan.nannan@yahoo.com

Rudi van Els
University of Brasilia, Campus Universitário Darcy Ribeiro, Brasília, Brazil
rudi@unb.br

Abstract. *The work presented in this paper is the result of a test project conducted in 2013 spanning a period of six months at the University of Brasilia (UnB) in collaboration with the Anton de Kom University of Suriname (AdeKUS). The aim of said project was to firstly experimentally determine the performance characteristics of a pico hydro turbine manufactured by Indalma Industries Inc. (3I), a company based in Brazil. As a second objective, a computational fluid dynamics (CFD) analysis was done to qualitatively identify, as a first assessment, the regions of flow losses in the turbine, and the interaction in the stator-rotor transition region. The experimental campaign at UnB yielded the following results, viz. the performance characteristics of the turbine in terms of the power, flow and efficiency as a function of the rotational speed of the shaft, the optimum efficiency of around 68.5%, as well as the turbine's specific speed. Moreover, the experimental results provided the boundary conditions for the CFD analyses. Using the experimental results as a point of departure, the numerical analyses showed that due to the absence of inlet guide vanes (IGV), high losses occur within the stator-rotor transition region. Although these losses are unquantified it is evident that they are significantly larger than comparable turbines, Dixon and Hall (2010). Furthermore, given the fact that for this specific turbine, approximately midway the shroud, it is non-smooth and additionally exceeds the typical value of 15 degrees for the flow angle, extra, yet avoidable, losses are present.*

Keywords: *CFD, Indalma turbine, Performance characteristics, Pico hydro-power*

1. INTRODUCTION

Turbines manufactured by Indalma Industries Inc. (3I) are developed for decentralized unattended power generation for isolated/remote communities (in the Brazilian Amazon hinterland), suitably adapted to the local context. Since 2000 over 1.5 MWe has been installed by 3I, providing electrical power to more than 2,200 families, van Els *et al.* (2010). In Suriname, contrary to the above mentioned Brazilian situation, the deployment (rate) of small scale hydro-power (i.e., less than 1 MWe) is significantly lower as is evident from the fact that: (1) the Poeketi micro hydro-power plant (30 kWe), is no longer functioning, and (2) the only other mini hydro-power plant, namely the one at Gran Olo Sula (150 kWe), is currently in the commissioning process. Given the fact that 15% of the population, mainly situated in the Surinamese hinterland, does not have adequate access to reliable electrical power, as well as Suriname's small-scale economy coupled to a weak world economy, climate-change challenges, Verlaan *et al.* (2008), and the green image that the country wishes to promote internationally, it is paramount to, among other things, conduct research on (pico) hydro-power for reliably and sustainably meeting local demand and accounting for the local context.

This paper presents the results of an experimental assessment and numerical analyses of a pico hydro turbine manufactured by 3I. The study is part of an informal broader joint research program between the Anton de Kom University of Suriname (AdeKUS) and the University of Brasilia (UnB) on sustainable development. The turbine under scrutiny is a unit fabricated by the 3I, and, based on its geometry, it can be classified as a Francis-type hydro turbine. Yet, it is distinct from a classical Francis turbine in the sense that it has neither IGV'S nor a water distributor. To understand the performance of the turbine under different conditions its characteristics need to be determined. For the specific turbine under scrutiny however, these characteristics are unknown. Given the latter, a test facility was designed, built and subsequently commissioned, allowing for measurements of the power output, rotational speed, flow rate and indirectly the efficiency, and the specific speed in order to classify the 3I turbine. Using the obtained data an assessment of the turbine's self regulating capacity, given the absence of a governor, was conducted. Anticipating that the outcome of the experimental phase would yield low efficiencies (this was confirmed after the experiments were conduced and the obtained data were post-processed), numerical analyses of the flow field through the turbine were performed, with the aim to compute and subsequently visualize the flow field in order to identify regions of losses. Knowledge of the flow field is relevant if the turbine is to be modified for improved efficiencies.

2. PICO HYDRO POWER

Internationally, pico hydro power (PHP) can be considered to be at the forefront of alternative and renewable energy technologies, due to its ability to derive energy from extremely low heads and flows, making this technology widely applicable, Lahimer *et al.* (2012). Furthermore, with the absence of large dams and serious deforestation, the environmental impact of such energy systems can be neglected.

Pico-hydro or family-hydro, is the smallest scale known in hydro power generation and, according to Williams and Simpson (2009), can be defined as having a capacity of less than 5 kW.

3. EXPERIMENTAL SETUP

Figure 1 shows a schematic overview of the experimental test setup. The facility was designed and built from the ground up, at campus Gama of the UnB, by a team of workers and students. Its intended use is to test various pico- and micro-turbine designs over a wide range of parameters encountered in the field, like the head at the inlet, the rotational speed of the shaft, the fluid flow rate and the pressure at the exit of the turbine, specifically if the turbine is equipped with a draft tube.

With reference to Fig. 1 the sequence of processes is as follows: (1) water is pumped from the *lower reservoir* to the *fill tube* and into the *down tube*. (2) If required, part of the water can be spilled through one of the *spill valves* into the *spill tube* and from there, back into the *lower reservoir*. (3) The remaining water in the *down tube* follows a path which leads to the turbine. (4) The water exiting the turbine is guided directly into the water in the *upper reservoir*. (5) Due to gravity, water flows from the *upper reservoir* to the *lower reservoir* thereby completing the cycle. Note that the use of two (2) reservoirs was a necessity in order to measure the flow rate using a V-notch weir.

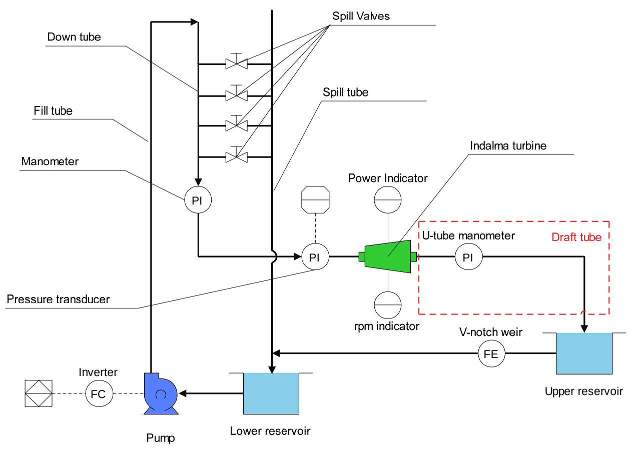

Figure 1. Schematic overview of the experimental test setup.

Furthermore, the test facility is equipped with instruments listed hereunder to either simulate and manipulate or measure respectively said field parameters or performance output variables:

- An inverter-controlled pump: the pump creates the necessary flow and head through the turbine and with the aid of the inverter these parameters can be varied nearly smoothly;

- Spill valves: these are parts of the piping arrangement that, in combination with the inverter, allow for varying the head at the turbine inlet;

- A de Prony brake: a dynamometer which uses friction to measure the amount of torque produced by the turbine. The de Prony brake consists of both a rotational speed sensor and strain gauges, which are used to measure forces produced by the turbine from which the torque can be deduced;

- A V-notch weir: an instrument used to measure the water flow rate. To obtain reliable data, measurements were taken at a time interval of 60 seconds. The uncertainty of this instrument was 0.2 l/s;

- Pressure gauges: both analog and digital instruments were used to measure the pressure at various parts of the facility to acquire therefrom the head and efficiency of the turbine. Figure 2 displays the digital pressure transducer at the inlet of the turbine.
- A data acquisition system (DAQ): to acquire the data measured by the sensors two DAQ systems were used, viz.: (1) CW552 kit DAQ, which, due to the microcontrollers software and hardware characteristics allow for usage with 64 kb of data memory and it has an 8-bit resolution and (2) the Arduino Uno R3 DAQ equipped with an ATmega32u4 microcontroller with a 10-bit resolution.

In order to accurately collect experimental data from the hydro turbine the total response of the system had to be determined. This means that it is needed to determine the maximum time which is required for each parameter to reach a steady state value within a variation of at most 2%, after a disturbance of at most 20% is applied (these percentages have been determined experimentally). From experiments it was found that the slowest response time emerged from the V-notch weir, and was around 40 seconds. To ensure reliable data a waiting period of circa a minute was used between measurements.

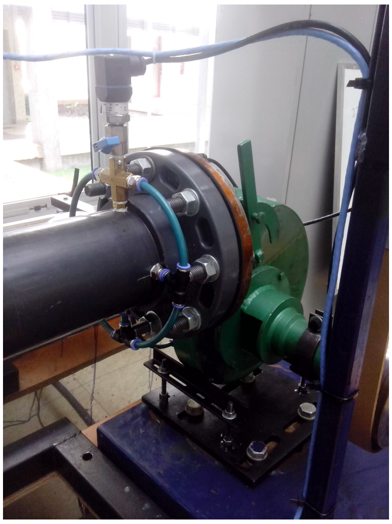

Figure 2. Pressure gauge at the turbine inlet.

The measurement procedure focused on acquiring data to calculate the differential energy potential across the turbine. The equation used for the calculations was derived from the general steady-flow energy equation, see Eq 2 presented in Sec. 4. Furthermore, the water head at the inlet of the turbine was kept constant. This was to approximate the conditions in which such a turbine should operate once installed in the field.

4. EXPERIMENTAL RESULTS

The shaft power (P) was calculated utilizing Equation 1, where r_{drum} is the radius of the de Prony brake drum, n the rotational speed and S_1 and S_2 the strain-force at either one of the sides of the drum.

$$P = |S_1 - S_2| r_{\mathrm{drum}} n \frac{2\pi}{60} \tag{1}$$

$$\left(\frac{p}{\gamma} + \frac{\alpha V^2}{2g} + z\right)_{\mathrm{in}} = \left(\frac{p}{\gamma} + \frac{\alpha V^2}{2g} + z\right)_{\mathrm{out}} + h_{\mathrm{friction}} - h_{\mathrm{pump}} + h_{\mathrm{turbine}} \tag{2}$$

The equation to determine the effective head was derived from the steady flow energy equation (Eq. 2, White (2011)).The friction losses included in Eq. 2, can and must be neglected when this equation is used to determine the effective head (H_{E}) for calculating the specific speed of a turbine. This is in consideration of the fact that the specific speed is a quantitative value which enables the designer to choose a turbine based on the available conditions at the location of installation, and therefore only the kinetic energy and potential energy at the inlet and the outlet are of importance. Equation 2 was subsequently simplified to Equation 3, where p_{in} is the inlet pressure, γ is the specific density of water (i.e., the density multiplied by the gravitational acceleration), g the acceleration of gravity, $\dot{Q}$ is the water flow rate, d is the tube diameter, and z_{out} is the distance between the turbine axis and the outlet water level.

$$H_{\mathrm{E}} = \frac{p_{\mathrm{in}}}{\gamma} + \frac{8\dot{Q}^2}{g\pi^2}\left(\frac{1}{d_{\mathrm{in}}} - \frac{1}{d_{out}}\right) + z_{\mathrm{out}} \tag{3}$$

Lastly, the overall efficiency (η_{tot}) was calculated with Equation 4, Choi *et al.* (2013)

$$\eta_{\mathrm{tot}} = \frac{P}{\gamma \dot{Q} H_{\mathrm{E}}} \tag{4}$$

4.1 Submerged draft tube vs non-submerged draft tube

In Fig. 3 the power curve of the turbine has been plotted at 5.5 m head and at two different turbine outlet conditions. A polynomial of the third order was used to fit these data points. A third-order polynomial was suitable because according to theory the power output is proportional to n^3. The dashed lines show results of a non-submerged-draft-tube condition and the continuous lines indicate the contrary. It follows from Fig. 3 that the 3I turbine has a higher power output and consequently a higher total efficiency if the draft tube is fully submerged in water as opposed to a non-submerged case. Although only a single graph is shown, this is consistently observed with all of the investigated inlet heads.

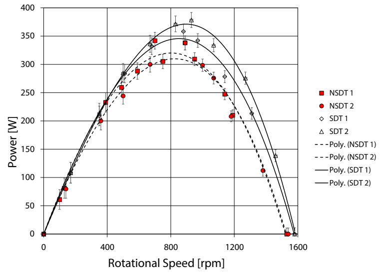

Figure 3. Comparison of power output between the submerged draft tube condition (SDT) and the non-submerged draft tube condition (NSDT). *The data in the graph was acquired at a head of 5.5 m.

Figure 3 indicates that the 3I turbine is more likely to be a reaction turbine than an action turbine. Although the power and efficiency were considerably higher with a submerged draft tube, care should be taken when choosing a draft tube design, because according to Harvey *et al.* (2013), the use of draft tubes for reaction turbines requires knowledge of its cavitation limits.

4.2 Performance characteristics of the 3I turbine

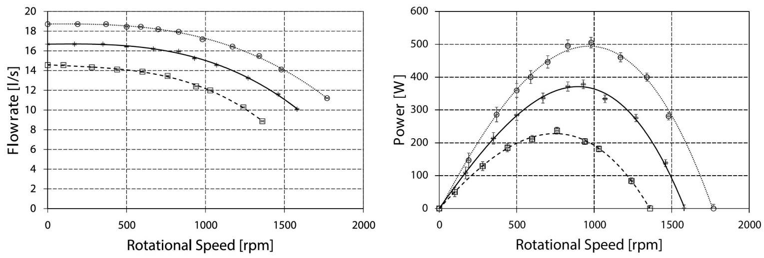

Figure 4. Flow and power curve of the 3I turbine at different heads.

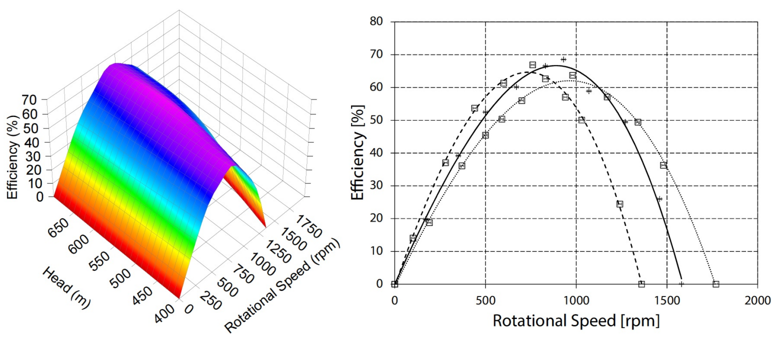

Figure 5. Efficiency curve of the 3I turbine at 4 m, 5.5 m and 7 m head.

Figures 4 and 5 show the experimentally obtained characteristic curves at different heads for respectively the flow and power and the efficiency.

4.2.1 Best efficiency point

The total efficiency curves of the experimental setup with the 3I turbine have been plotted in efficiency hill curves shown in Fig. 5. Remark that the head in this figure is not the effective head, but rather the head measured at the manometer.

The BEP of the pico hydro 3I turbine (on the used experimental setup) was measured at a head of 5.5 m. The water flow rate and rotational speed at the BEP was used to calculate the specific speed of the turbine.

4.2.2 Specific speed

The specific speed (Ω_{sp}) was calculated using Eq. 5, leading to a value of 0.67 rad.

$$\Omega_{\mathrm{sp}} = \frac{\Omega(P/\rho)^{\frac{1}{2}}}{(gH_{\mathrm{E}})^{\frac{5}{4}}} \tag{5}$$

Where Ω is the angular speed at B.E.P. and ρ the density of water.

Using the corresponding specific-speed graph, refer to Fig. 6, the specific speed of the 3I turbine lies within the range of the Francis turbine. (Note: Fig. 6 is log scaled, the 3I turbine lies only 15% higher than the lowest-specific-speed range of 0.4 rad for Francis turbines.)

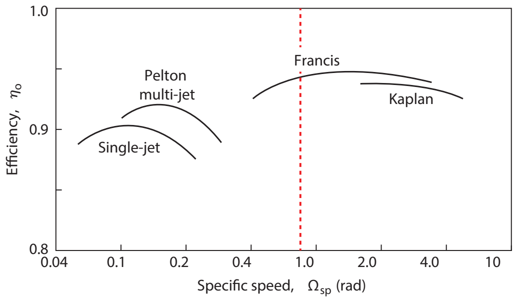

Figure 6. Typical Design Point Efficiencies of Pelton, Francis, and Kaplan Turbines Dixon and Hall (2010).
The dashed red line indicates the calculated specific speed of the 3I turbine.

4.2.3 Self regulating capacity

Consider a hypothetical case of a 3I turbine installation whereby the available head pressure is of the order of 5.5 m, the draft tube is submerged in water, and where the power curve is equivalent to that shown in Fig. 3. Moreover, the operation point would be 75% of the runoff speed (according to 3I's operation conditions this equals 1185 rpm). Suppose next that a commonly available 4 pole synchronous generator would be used (a synchronous generator with an automatic voltage regulator (AVR) is highly recommended). This would then imply that the rotational speed of the generator would have to be 1800 rpm. Such a condition could be achieved with a transmission ratio of $1800\ \mathrm{rpm}/1185\ \mathrm{rpm} \approx 1.5$. One of the disadvantages of the off-the-shelf synchronous generators is however, that the maximum safe speed ratio is often unknown. This is, among other reasons, why a larger capacity synchronous generator would be used for these conditions (usually upto 60% larger).

For a micro-hydro system where there are no transformers or induction motors, voltage limits of +7% to -10% and frequency (f) limits of +10% to -5% of the rated value are recommended Harvey *et al.* (2013). This implies that the generator would have to be regulated between $12057\ \mathrm{Hz}/4 = 1710\ \mathrm{rpm}$ to $12066\ \mathrm{Hz}/4 = 1980\ \mathrm{rpm}$ and that the turbine would have to auto regulate between $1710\ \mathrm{rpm}/1.5 = 1140\ \mathrm{rpm}$ to $1980\ \mathrm{rpm}/1.5 = 1320\ \mathrm{rpm}$. The self regulating capacity in terms of rotational speed could then be calculated by: $(f_{max} - f_{min})/f^{\star}100\% \approx 15\%$. And The self regulating capacity in terms of power could then be calculated by: $(P_{max} - P_{min})/P^{\star}100\% \approx 30\%$.

Although the self-regulating capacity is only -23.8% to +4.8% in terms of shaft power output, the turbine displays a stable operating condition, (due to the naturally occurring negative feedback loop) without any mechanical or electronic control system, therefore, operation under said interval is less expensive and less prone to catastrophic failure.

5. NUMERICAL SIMULATION

By applying the CFD techniques on the pico hydro turbine manufactured by 3I, the specific locations of losses can be determined through analysis of the streamline patterns. In principle the losses can also be quantified using rigorous thermodynamics. The tool used to model the turbine and to solve the associated mathematical set of equations for the

Speed	Flow Rate	Power	Outlet Press. (abs.)	Efficiency	Head (inlet)
930 rpm	15.249 $\mathrm{m}^3 \cdot \mathrm{s}$	379 W	99657.87 Pa	68.5	3.1 m

Table 1. Experimentally measured data at BEP.

flow field analyses is ANSYS CFX, in short ANSYS. This software package was selected solely because the authors have experience with the program and therefore they have more control over the setup of the simulation. The pre-processing was done using ANSYS server programs of which in-depth specification will be given further in this document. The simulation was performed at a single steady state operating point of which the data were measured experimentally and given in Table 1.

5.1 Creating the geometry

The geometry of the 3I Turbine was partially modeled using the CAD software SolidWorks, whereas the topology of the rotor was generated using BladeGen. The model includes the hub, blades, outlet and shroud.

5.2 Mesh generation

The fluid domain of the rotor passages and the shroud where meshed using respectively ANSYS TurboGrid and ANSYS ICEM CFD. The element size near the wall of the rotating frame is calculated with the aid of an initially guessed Reynolds number of $1 \cdot 10^6$, which corresponds with a y^+ of approximately 183 within the fluid passage. Remark that no exact study has been done to determine the Reynolds number of the flow through the rotor passage and thus the height of the turbulent boundary layer is unknown, Pasquale (2014). The shroud is meshed using tetra/prism mesh while the fluid passages of the rotor where meshed using H-mesh blocks. The final generated three-dimensional mesh was comprised of 4,467,417 elements.

5.3 Preprocessing of the numerical simulation

The turbulence model used for this simulation is the Shear Stress Transport (SST) model. This model best represents turbo machinery, a claim supported by many CFD practitioners (see e.g. cfd-online.com). To verify this claim, the second turbulence model option, k-ϵ, was applied, which indeed failed to converge.

6. NUMERICAL RESULTS

In the present study solely the BEP was used as operating point, stating that at this point the fluid within the turbine reaches its maximum momentum transfer per unit power and it can thus be assumed that the streamlines resulting from this simulation give a valid representation as to where the regions of losses are located. The velocity profile at the inlet of casing is uniform and evenly distributed. From this point on, the stream gradually transforms into a vortex-free flow as it advances towards the leading edge (LE) of the rotor, as shown in Fig. 7.

The approximately smooth and uniform pressure distribution in Fig. 7 around the rotor, as observed in a stationary reference frame, yields a uniform velocity vector field and therefore the flow exiting the volute into the rotor is uniform all around. Conversely, for the rotor there are clear locations where there is a higher pressure gradient than elsewhere, see Fig. 8. From the viewpoint of a rotating reference frame, this is caused by a mismatch between the angle of attack and the rotor blade angle, as is elucidated in Fig. 7

As Fig. 9 illustrate the pressure distribution over respectively the pressure- and suction side of rotor vane is not uniform. This inconsistency is more pronounced at the LE of the pressure side. Considering an ideal rotor vane, uniformity of the pressure distribution is desired, since the pressure contour indirectly influences the delivered torque. This case is made more obvious with the aid of Fig. 10 where the pressure difference between the pressure- and suction side is illustrated. The initially lower dotted-line represents the pressure curve of the suction side, whereas the upper dotted-line represents that of the pressure side. Analyzing this plot shows that only about the first 30% of the blade (with respect to the streamline at a span of 0.5) is suitably utilized, whereas the latter part is not. The condition is exacerbated, since the subsequent 30% of the blade results in a power loss, as can be inferred from the crossing of the dotted-lines over each

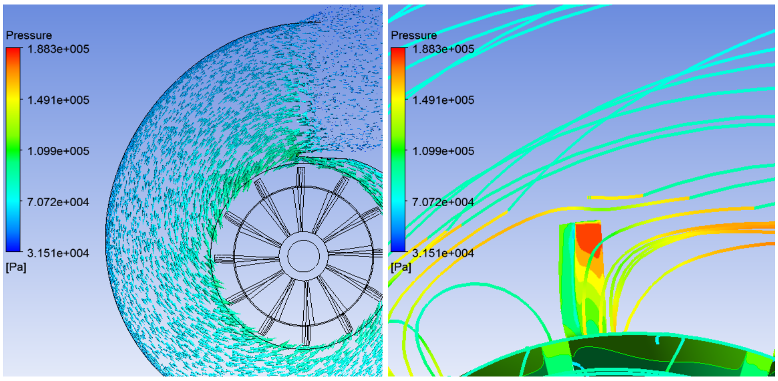

Figure 7. Velocity vector field and Flow field collision at respectively the "outlet" of the volute casing and at the LE of a rotor vane.

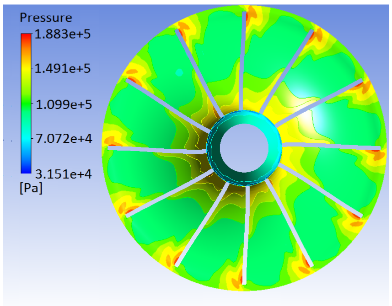

Figure 8. Pressure field plotted against the rotor hub.

other. This can be explained due to detachment of the boundary layer as a consequence of flow vortices.

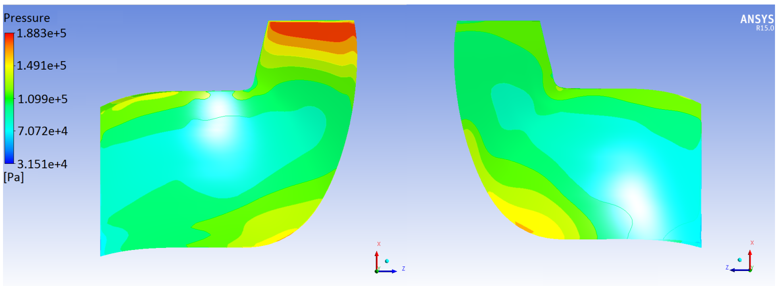

Figure 9. Pressure- and suction side of a single rotor vane.

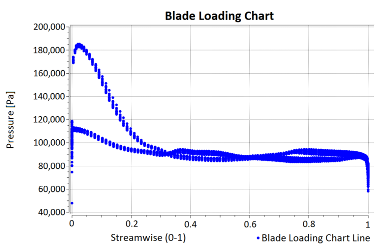

Figure 10. Blade loading chart.

7. CONCLUSION

7.1 characteristics of the indalma turbine

Comparing the characteristics of the Francis turbine with the experimentally obtained characteristics of the 3I turbine, one can argue that the initial hypothesis, formulated in Sec. 1is validated. That is to say that indeed the 3I turbine is of the Francis type. This finding is confirmed with the specific speed according to Eq. 5 and Fig. 6. Additionally, it has been found from the experiments that the maximum power output at the shaft of the 3I turbine under investigation is of the order of 530 W at $\sim$1050 rpm with a total efficiency of approximately 64%.

7.2 Regions of losses

As can be concluded or rather confirmed, is that the efficiency of this turbine proves to be rather low.[1] The cause hereof is a summation of errors/deviations of the turbine's geometry. Starting with the turbine volute, which proves to have a fairly smooth scroll casing wherein losses are negligible, however, due to the absence of IGV's within the volute, the angle of attack at the LE is rather large. Consequently the first 30% of the blade gains its momentum solely through drag forces (impulse). When analyzing reaction turbines, momentum transfer due to drag is seen as inefficient. The desirable situation would be to create a momentum transfer due to lift forces and in this way more energy can be extracted from the fluid medium resulting a greater blade torque. Secondly, it can be concluded that due to the incorrect design of the rotor vane and also a large angle of attack at the LE, boundary layer detachment is observed at approximately 30% along the streamline direction, implying so to say that up to 70% of the blade area is unused. Thirdly, the streamlines at the shroud do not exhibit a smooth transition from LE to TE, resulting in a sudden deflection of the streamlines and therefore an unnecessary power loss. Finally, it can be concluded that although the turbine under scrutiny is of the mixed flow type, the simulation results show that virtually all energy is extracted due to momentum transfer and this potentially explains why this turbine lies so near the Pelton region.[2]

8. REFERENCES

Choi, H.J., Zullah, M.A., Roh, H.W., Ha, P.S., Oh, S.Y. and Lee, Y.H., 2013. "Cfd validation of performance improvement of a 500 kw francis turbine". *Renewable Energy*, Vol. 54, No. 0, pp. 111 – 123. ISSN 0960-1481. URL http://www.sciencedirect.com/science/article/pii/S0960148112005198.

Dixon, S.L. and Hall, C.A., 2010. *Fluid Mechanics and Thermodynamics of Turbomachinery*. Elsevier, 6th edition.

Harvey, A., Brown, A., Hettiarachi, P. and Inversin, A., 2013. *Micro-Hydro Design Manual*. Practical Action Publishing.

Lahimer, A., Alghoul, M., Sopian, K., Amin, N., Asim, N. and Fadhel, M., 2012. "Research and development aspects of pico-hydro power". *Elsevier*, Vol. 16, pp. 5861–5878.

Pasquale, D., 2014. "Expert advice".

van Els, R.H., Vianna, J. and Brasil, A., 2010. "Eletrificação rural em santarém: contribuição das microcentrais hidrelétricas". *Revista Brasileira de Energia*, Vol. 16, No. 2, pp. 35–46.

Verlaan, R., Ajodhia, V., Balijn, J., Humphrey, B., Prado, B. and dos Ramos, O., 2008. "Suriname power sector assessment and alternatives for its modernization (atn/sf-9038-su) - preliminary assessment report". Technical report, Ministry of Natural Resources of Suriname.

White, F.M., 2011. *Fluid Mechanics*. McGraw-Hill Companies, 7th edition.

Williams, A. and Simpson, R., 2009. "Pico hydro - reducing technical risks for rural electrification". *Elsevier*, Vol. 34.

9. RESPONSIBILITY NOTICE

The following text, properly adapted to the number of authors, must be included in the last section of the paper:
The authors are the only responsible for the printed material included in this paper.

[1] Typically efficiencies of such turbines can reach beyond the order of 90% as opposed to the value of roughly 68.5% for this device, Dixon and Hall (2010).

[2] The 3I turbine lies approximately 15% to the right of the Pelton-Francis border.